Designing a Transition State Analogue for the Disfavored Intramolecular Michael Addition of 2-(2-Hydroxyethyl)acrylate Esters

Manuel Arnó,* Luis R. Domingo,* and Juan Andrés†

Departamento de Química Orgánica, Universidad de Valencia, Dr. Moliner 50, 46100 Burjassot, Valencia, Spain, and Departament de Ciències Experimentals, Universitat Jaume I, Apartat 224, 12080, Castelló, Spain

Received July 12, 1999

The rate-determining steps for the intramolecular 1,2 and 1,4 addition reactions in basic medium of methyl 2-(2-hydroxyethyl)acrylate to give the corresponding γ-lactone and tetrahydrofuran, respectively, have been characterized at the ab initio HF/6-31+G* calculation level. Transition structures have been located on the reactive potential energy surface. The intramolecular 1,2 addition corresponds with the favored pathway due to the small value of the attack angle of the alkoxy group on the conjugated position along the pathway for the intramolecular 1,4 addition. Acid/base catalyst effects have been modeled by the inclusion of methylammonium cation and formiate anion forming hydrogen bonds with the carbonyl and the hydroxyl group, respectively. The different geometrical parameters, charge distribution, and shape of the molecular electrostatic potential for the corresponding acid/base-catalyzed transition structures allow us to select an adequate transition state analogue to favor the intramolecular 1,4 addition reaction with respect to the 1,2 one.

Introduction

The synthesis of catalysts with tailored specificities and desirable properties is a challenging problem to both chemists and biologists alike. A key element in the design of catalytic systems is the rational generation of substrates capable of discriminating synthetic routes with high selectivity. This research field has begun to focus on selective chemical transformations that are difficult to achieve via existing chemical methods, including disfavored chemical reactions.[1] In particular, Houk and al.[2] have defined a theozyme as "an array of functional groups in a geometry predicted by theory to provide transition state stabilization". They can be employed to better understand biological catalysts or to design new inhibitors, haptens, or synthetic catalysts.

For reactions under kinetic control in which a number of reaction products are possible, the product distribution reflects the relative energies of each transition structure (TS). The generation of the appropriate substrates can be pursued by taking into account al least the following devices: (i) stereoelectronic features of their respective TSs and (ii) the fact that the outcome of the chemical transformations can be controlled by their energy requirements involved in orienting reaction patters and the selection of appropriately positioned residues into the combining site.

Transition state analogues (TSA) have been produced for more than 50 reactions involving conversion of either macromolecular or simple chemical substrates to products.[3,4] TSAs can be used in an active manner to provide a practical route to synthetic organic chemistry and thereby allow one test in practice theoretical models for selected chemical reactions. The majority of these reactions are either unimolecular or ester hydrolysis reactions, and the number of antibodies which catalyze reactions resulting in formation of carbon−carbon bonds is relatively small.[5−10]

Bond formation between carbon atoms is a keystone of synthetic organic chemistry, and the Michael addition of weak acids to electron deficient double bonds is among the most useful of such reactions.[11] A related synthetic reaction is the intramolecular attack of oxygenated acid groups to electron deficient double bonds to give heterocyclic systems. The tetrahydrofuran system, which is present in several natural products with biological activity as polyether antibiotics,[12] could be formed via this mode of intramolecular Michael addition. However, Baldwin's rules[13,14] penalize the formation of the aforementioned five-membered rings via an intramolecular process.[15] Thus, alcohol **1** upon treatment with a variety of bases closed efficiently and cleanly to γ-lactone **2**, with no traces of tetrahydrofuran **3** (see Scheme 1).[15]

(1) Thomas, N. R. *Nat. Prod. Rep.* **1996**, 479.
(2) Tantillo, D. J.; Chen, J.; Houk, K. N. *Current Opin. Chem. Biol.* **1998**, *2*, 743.
(3) Benkovic, S. J. *Annu. Rev. Biochem.* **1992**, *61*, 29.
(4) Schultz, P. G.; Lerner, R. A. *Acc. Chem. Res.* **1993**, *26*, 391.
(5) Hilvert, D. *Acc. Chem. Res.* **1993**, *26*, 552.
(6) Gouverneur, V. E.; Houk, K. N.; de Pascual-Teresa, B.; Beno, B.; Janda, K. D.; Lerner, R. A. *Science* **1993**, *262*, 204.
(7) Braisted, A. C.; Schultz, P. G. *J. Am. Chem. Soc.* **1994**, *116*, 2211.
(8) Chen, Y.; Reymond, J.-L.; Lerner, R. A. *Angew. Chem., Int. Ed. Engl.* **1994**, *33*, 1607.
(9) Li, T.; Janda, K. D.; Ashley, J. A.; Lerner, R. A. *Science* **1994**, *264*, 1289.
(10) Cook, C. E.; Allen, D. A.; Miller, D. B.; Whisnant, C. C. *J. Am. Chem. Soc.* **1995**, *117*, 7269.
(11) Perlmutter, P. *Conjugate Addition Reactions In Organic Syntesis*; Pergamon Press: New York, 1992.
(12) Katritzky, A. R.; Rees, C. W.; Scriven, E. F. V. *Compr. Heterocycl. Chem.* **1996**, *2*, 385−386.
(13) Baldwin, J. E. *J. Chem. Soc., Chem. Commun.* **1976**, 734.
(14) Baldwin, J. E.; Thomas, R. C.; Kruse, L. I.; Silberman, L. *J. Org. Chem.* **1977**, *42*, 3846.
(15) Baldwin, J. E.; Cuttin, J.; Dupont, W.; Kruse, L.; Silberman, L.; Thomas, R. C. *J. Chem. Soc., Chem. Commun.* **1976**, 736.

10.1021/jo991117c CCC: $18.00
Published on Web 11/19/1999

Scheme 1

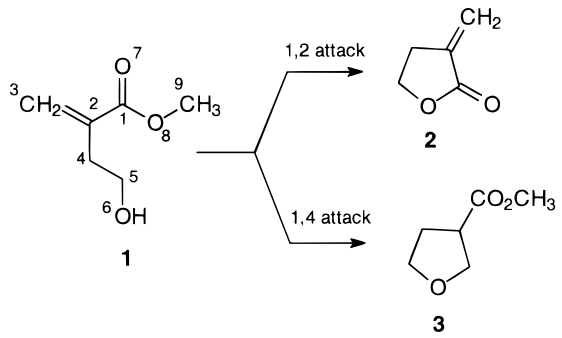

Scheme 2

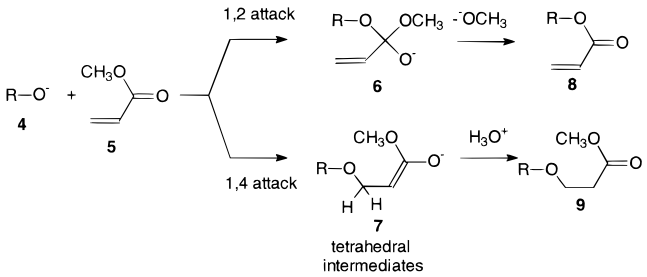

The present theoretical study was undertaken in order to provide knowledge about the TS corresponding to the rate-determining steps of the aforementioned reactions, to gain insight into the origins of catalysis of the reactions, and to determine whether theoretical methods could be used to design TSAs which more closely resemble to TS for the disfavored intramolecular Michael addition of methyl 2-(2-hydroxyethyl)acrylate **1** to give tetrahydrofuran **3** instead of the expected γ-lactone **2**. In essence, the issue concerns the ability of a suitably programmed model system to intercede at or near the TS to alter the energy balance in favor of the otherwise disfavored reaction pathway. Herein we demonstrate this principle by generating model systems that favor a disfavored chemical transformation.

Computing Methods

All geometry optimizations of reactants and TSs were performed with the Gaussian 94 suite of programs[16] at the RHF/6-31+G* level. The potential energy surfaces (PESs) for the intramolecular 1,2 and 1,4 additions of **1** have been calculated in detail. Stationary points have been located without any geometry restriction and have been characterized through the calculation of the force constants matrix by ensuring that they correspond to minima or saddle points on the PES; i.e., they have zero or one and only one imaginary frequency, respectively. The optimizations were carried out using the Berny analytical gradient optimization method.[17,18] Optimized geometries of all stationary points on PESs are available from the authors. The electronic structures of stationary points were analyzed by the natural bond orbital (NBO) method.[19,20] Electrostatic potential surfaces were created using SPARTAN.[21] The electrostatic potential for each structure was mapped onto a total electron density surface contoured at 0.002 e/au^3.

The enthalpy and entropy changes are calculated from standard statistical thermodynamic formulas.[22,23] The computed values of activation enthalpies, entropies, and Gibbs energies have been estimated by means of the RHF/6-31+G* potential energy barriers along with the harmonic frequencies. These frequencies have been scaled by 0.91.[24] The activation Gibbs energies have been computed at 298.15 K. Single point calculations at B3LYP/6-31+G*//HF/6-31+G* and MP2/6-31+G*//HF/6-31+G* have been carried out in order to check the energetic results.

Results and Discussion

First, the geometries for the TSs associated with the intramolecular 1,2 and 1,4 additions of methyl 2-(2-hydroxyethyl)acrylate **1** in basic medium with formation of **2** and **3**, respectively, are characterized. Second, the acid/base catalyst effects on the course of these additions are considered; we have explored the role of the correct positioning of the acid/base residues to find the arrangement of the catalysts that favors the intramolecular Michael process (intramolecular 1,4 addition). Finally, with the aim of inducing catalytic antibodies by immunization, we sought to design an accurate and conformationally stable TSA to favor the formation of tetrahydrofuran system **3** instead of the expected γ-lactones **2**.

(i) Study of the Intramolecular 1,2 and 1,4 Additions of Methyl 2-(2-Hydroxyethyl)acrylate 1 in Basic Medium. The 1,2 and 1,4 addition reactions of an alcohol to an α,β-unsaturated ester are stepwise processes where the first and rate-determining step is a nucleophilic attack of corresponding alkoxide **4** on the 2 or 4 position of the α,β-unsaturated ester **5** to give two tetrahedral intermediates, **6** or **7** (see Scheme 2). These intermediates afford the final products: **8** via the alkoxy elimination or **9** by a protonation of the corresponding enolate. Thus, in the present study we have studied the first and rate-determining step of these processes associated with the formation of **6** or **7**.

Methyl 2-(2-hydroxyethyl)acrylate **1** has been deprotonated by following the experimental conditions (basic medium), since the reaction does not take place in neutral conditions because the alcohol group is a poor nucleophile. Free chain rotations around C2−C4, C4−C5, and C5−O6 single bonds allow the presence of different alkoxy ester conformers, with two of them corresponding to the alkoxy ester precursors of the two competitive channels, in a narrow range of relative energy, around 0.3 kcal/mol. This fact allows us to select a unique alkoxy ester precursor, **1-D**, for the 1,2 and 1,4 additions as reference to obtain the activation parameters. Two transitions structures, **TS1-D** and **TS2-D**, were located

(16) Frisch, M. J.; Trucks, G. W.; Schlegel, H. B.; Gill, P. M. W.; Johnson, B. G.; Robb, M. A.; Cheeseman, J. R.; Keith, T.; Petersson, G. A.; Montgomery, J. A.; Raghavachari, K.; Al-Laham, M. A.; Zakrzewski, V. G.; Ortiz, J. V.; Foresman, J. B.; Cioslowski, J.; Stefanov, B. B.; Nanayakkara, A.; Challacombe, M.; Peng, C. Y.; Ayala, P. Y.; Chen, W.; Wong, M. W.; Andres, J. L.; Replogle, E. S.; Gomperts, R.; Martin, R. L.; Fox, D. J.; Binkley, J. S.; Defrees, D. J.; Baker, J.; Stewart, J. P.; Head-Gordon, M.; Gonzalez, C.; Pople, J. A. *Gaussian 94*, Gaussian, Inc., Pittsburgh, PA, 1995.

(17) Schlegel, H. B. *J. Comput. Chem.* **1982**, *3*, 214.

(18) Schlegel, H. B. Geometry Optimization on Potential Energy Surface. In *Modern Electronic Structure Theory*; Yarkony, D. R., Ed.; World Scientific Publishing: Singapore, 1994.

(19) Reed, A. E.; Weinstock, R. B.; Weinhold, F. *J. Chem. Phys.* **1985**, *83*, 735.

(20) Reed, A. E.; Curtiss, L. A.; Weinhold, F. *Chem. Rev.* **1988**, *88*, 899.

(21) SPARTAN V4.0, Wavefunction, Inc., 1995, 18401 Von Karman Avenue, #370, Irvine, CA 92715.

(22) Hehre, W. J.; Radom, L.; Schleyer, P. v. R.; Pople, J. A. *Ab initio Molecular Orbital Theory*; Wiley: New York, 1986.

(23) Jorgensen, W. L.; Lim, D.; Blake, J. F. *J. Am. Chem. Soc.* **1993**, *115*, 2936.

(24) Grev, R. S.; Janssen, C. L.; Schaefer, H. F., III. *J. Chem. Phys.* **1991**, *95*, 5128.

Table 1. Total Energies (au) and Relative Energies[a] (kcal/mol, in parentheses) of the Stationary Points for the Intramolecular 1,2 and 1,4 Additions of 1

	HF/6-31+G*		B3LYP/6-31+G*//HF/6-31+G*		MP2/6-31+G*//HF/6-31+G*	
1-D	−456.998221		−459.727333		−458.331329	
1-A	−553.222112		−556.574646		−554.828687	
1-B	−645.855748		−649.577533		−647.671664	
1-AB	−741.553014		−745.921316		−743.673357	
TS1-D	−456.992374	(3.7)	−459.728699	(−0.9)	−458.334997	(−2.3)
TS2-D	−456.974795	(14.6)	−459.722747	(2.9)	−458.324315	(4.4)
TS1-A	−553.147213	(47.0)	−556.500314	(46.6)	−554.756832	(45.1)
TS2-A	−553.147971	(46.5)	−556.516040	(36.8)	−554.763480	(40.9)
TS1−B	−645.797996	(36.2)	−649.534674	(26.9)	−647.634343	(23.4)
TS2−B	−645.791939	(40.0)	−649.533677	(27.5)	−647.626745	(28.2)
TS1-AB	−741.544282	(5.5)	−745.923847	(−1.6)	−743.677175	(−2.40)
TS2-AB	−741.517993	(22.0)	−745.902717	(11.7)	−743.643880	(18.5)

[a] Relatives to the corresponding reactant; **1-D** (in basic medium), **1-A** (acid-catalyzed reactions), **1-B** (base-catalyzed reactions), and **1-AB** (acid/base-catalyzed reactions).

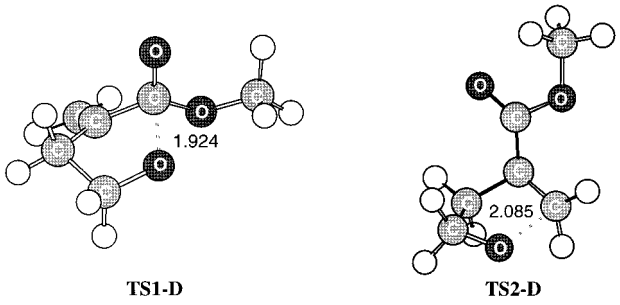

Figure 1. Selected geometrical parameters for the transition structures **TS1-D** and **TS2-D** corresponding to the intramolecular 1,2 and 1,4 additions of **1** in basic medium. The lengths of the C−O forming bonds involved in the reaction are given in angstroms.

and properly characterized on PESs for these pathways, respectively. The geometries of these stationary points are depicted in Figure 1 while the relative energies are summarized in Table 1. **TS1-D** is more stable than **TS2-D**, 10.9 kcal/mol, the former having a very low potential energy barrier (PEB), 3.7 kcal/mol. Therefore, in basic medium, only the γ-lactone **2** is obtained and Baldwin's rules are fulfilled.[13,14]

To analyze the effects of geometical strains in these intramolecular additions, we have studied the TSs associated with the intermolecular 1,2 and 1,4 additions of the methoxy anion **4** (R = CH_3) to methyl acrylate **5** (see Scheme 2). For these processes, the TS for the 1,4 addition is only 3.4 kcal/mol more energetic than for the 1,2 one. The values of the attack angles are 104.8° and 114.9°, respectively. Bayly and Grein[25] have studied the intermolecular Michael addition of the methoxy anion to methyl vinyl ketone, finding an *anti* attack angle of 117.9° at the corresponding TS. Therefore, the lower value of the *syn* attack angle required along the intramolecular 1,4 addition, 96.6°, accounts for the larger energy of **TS2-D** with respect to **TS1-D**.

The lengths of the C−O forming bonds in **TS1-D** and **TS2-D** are 1.924 Å (C1−O6) and 2.085 Å (C3−O6), respectively. In addition, the bond order[26] values of these forming bonds are 0.32 and 0.29, respectively; therefore, the 1,2 attack is slightly more advanced than the 1,4 one.

The values of activation enthalpies, entropies, and Gibbs energies corresponding to the two competitive reactive channels are summarized in Table 2. The

(25) Bayly, C. I.; Grein, F. *Can. J. Chem.* **1989**, *67*, 2173.
(26) Wiberg, K. B. *Tetrahedron* **1968**, *24*, 1083.

Table 2. Activation Enthalpies (in kcal/mol), Entropies (in kcal/mol·K) and Gibbs Energies (in kcal/mol) Computed at 298.15 K and 1 atm for the Intramolecular 1,2 and 1,4 Additions of 1 in Basic Medium

	$\Delta H^{\#}$	$\Delta S^{\#}$	$\Delta G^{\#}$
TS1-D	3.05	−5.08	4.57
TS2-D	14.19	−5.79	15.92

inclusion of the zero-point energy and thermal contributions to the PEBs leads to a small decrease in the activation enthalpy for **TS1-D** and **TS2-D**. Moreover, the negative values of the corresponding activation entropies, −5.1 and −5.8 kcal/mol·K, respectively, lead to a small increase of the values of the activation Gibbs energies relatives to the PEBs. The activation Gibbs energies for these intramolecular attacks are 4.6 and 15.9 kcal/mol, respectively. The closer values of activation Gibbs energies and PEBs allow us to use the latter values in this study.

(ii) Acid/Base Catalytic Effects on the Intramolecular 1,2 and 1,4 Additions of 1. The next step was the study of the presence of acid and base residues on the two possible intramolecular addition reactions of methyl 2-(2-hydroxyethyl)acrylate **1**. These reactions can be catalyzed by both acid and base species. The former can protonate the O7 oxygen atom of the carbonyl group, yielding an increase of the electrophilic character of C1 and C3 carbon atoms while the presence of a base can favor the proton abstraction process on the hydroxyl group, increasing the nucleophilic character of the O6 oxygen atom of the alcohol group. In enzymatic environments the acid−base conditions must be very mild, and no strong acids or bases can be used; therefore, the formate anion and methylammonium cation have been selected for modeling the carboxylate and ammonium fragments, respectively.

Three catalytic models have been considered: (i) acid catalyst, where a hydrogen of the ammonium group is hydrogen-bonded to the O7 oxygen atom of the carbonyl group, (ii) base catalyst, an oxygen atom of the formiate anion is hydrogen-bonded to the H atom of the hydroxyl group, O6-H, and (iii) acid/base catalyst, where both ions are hydrogen-bonded. In the first step, the hydrogen-bond distances are optimized while in the second step the remaining geometrical parameters were fully optimized. Thus three reactants, **1-A**, **1-B**, and **1-AB**, and six TSs, **TS1-A**, **TS2-A**, **TS1-B**, **TS2-B**, **TS1-AB**, and **TS2-AB**, have been characterized. The geometries of **1-AB**, **TS1-AB**, and **TS2-AB** are depicted in Figure 2 while the relative energies are summarized in Table 1.

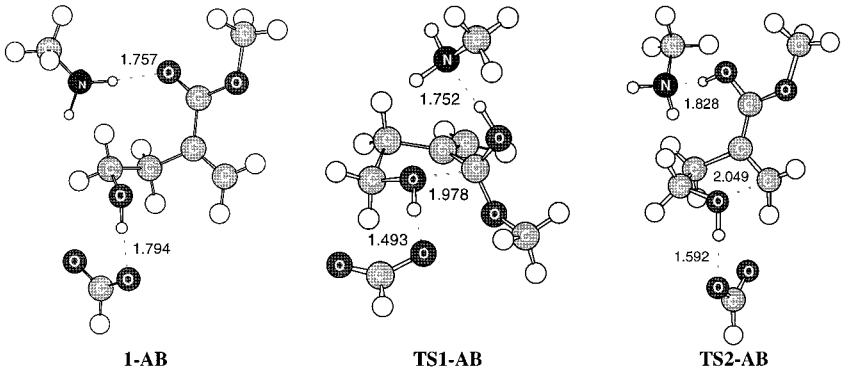

Figure 2. Selected geometrical parameters for **1-AB** and for the transition structures **TS1-AB** and **TS2-AB** corresponding to the acid/base-catalyzed intramolecular 1,2 and 1,4 additions of **1**. The lengths of the C−O forming bonds involved in the reaction are given in angstroms.

Scheme 3. Model Systems Associated with the Catalyzed Acid/Base Intramolecular 1,2 and 1,4 Additions of 1

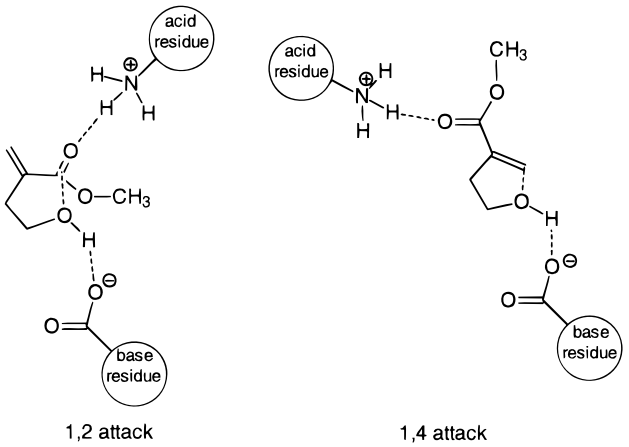

An analysis of the energetic results points out that the values of PEBs for the acid- and base-catalyzed processes are lower than those for the uncatalyzed process.[27] However, in the case of the double acid/base-catalyzed process, **TS1-AB** and **TS2AB**, the corresponding PEBs decrease drastically. Now, the PEB for **TS1-AB** is similar to that for **TS1-D**, while for **TS2-AB** is around 7 kcal/mol higher than that for **TS2-D**. These energetic results are very promising for the antibody catalyst design because the spatial demands of both acid and base catalysts can discriminate both additions. The relative energies of the corresponding TSs can be modified, and preferential formation of the unexpected tetrahydrofuran **3** product can be obtained. The present results show that the key factor to obtaining an efficient catalytic function is associated with the precise positioning between reactant and the active acid/base residues (see Scheme 3).

At **TS1-A**, **TS2-A**, **TS1-B**, and **TS2-B** the lengths of the C1−O6 and C3−O6 forming bonds, in the range of 1.62−1.76 Å, are shorter than those for **TS1-AB** and **TS2-AB**, in the range 1.98−2.05 Å, the latter being closer to those at **TS1-D** and **TS2-D**. Moreover, for the acid-catalyzed processes, **TS1-A** and **TS2-A**, the lengths of the O7−H7 forming bonds, ca. 0.9 Å, indicate that the H7 atom of the ammonium group has been transferred while for the base-catalyzed processes the lengths of the O6−H6 breaking bonds indicate that at **TS1-B** (1.54 Å) the abstraction process is more advanced than that for **TS2-B** (1.01 Å). At the acid−base-catalyzed processes, **TS1-AB** and **TS2-AB**, the lengths of the O7−H7 forming bonds and the O6−H6 breaking bond are ca. 0.9 and 1.0 Å, respectively. Therefore, in these TSs H7 hydrogen atom have been transferred whereas the H6 atom of the hydroxyl group is not removed.

To establish the influence of electron correlation, single point calculations by the B3LYP/6-31+G* and MP2/6-31+G* computing methods have been carried out. The results are presented in Table 1. An analysis of the data shows that the relative energies among the different TS are dependent on the calculation method; however, a similar trend is obtained for these relative energies with the inclusion of acid, base, and acid/base catalysts. Moreover, although the inclusion of electron correlation favors the **TS2A** relative to the **TS1A**, the acid/base catalyst is necessary for the reaction to take place.

(iii) Theoretical Design of a TSA Based on the TS Geometry and Charge Distribution. In this section four TSAs are proposed to favor the intramolecular Michael addition with respect the 1,2 addition. This proposal is based on these target molecules acting as a template to direct the antibody to fold into the shape that complements it best. Therefore, it can discriminate one TS of the disfavored synthetic route from another. Two major factors have been considered to select the suitable TSAs: (i) the shape given by the geometry and (ii) the charge distribution displayed by the net atomic charge on the atomic centers and the molecular electrostatic potential (MEP). The first property ensures that the TSAs fulfill the appropriate geometric requirements while the second ones ensure that the TSAs will interact in a fashion similar to that of the TS. Thus, we have investigated a set of related electronic and geometrically related TSAs with **TS2-A′B′**, presenting here the four more relevant ones.[28] All proposed TSAs are substituted hydrogenated heterocycle systems, which simulates the geometrical features of **TS2-A′B′**, while the different substitutions on the ring approximate the charge distribution of TSAs to that of **TS2-A′B′**. Thus, the heteroatoms present on the heterocycle system, which have an

(27) Although the corresponding TSs for the uncatalyzed processes have not been found, since they take place along an alternative one-step mechanism, restricted geometry optimizations give very energetic processes; 45 and 56 kcal/mol, respectively.

(28) Evaluations of the similarity of the different proposed TSAs with **TS2-AB** have been carried out using the **TS2-A′B′**, which correspond to **TS2-AB** geometry without the presence of both acid and basic catalysts.

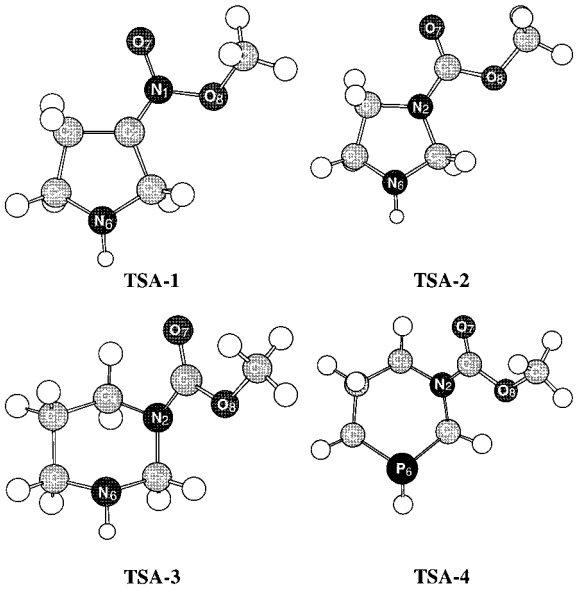

Figure 3. Geometries of the proposed TSAs.

acid hydrogen, promote the basic catalyst, while the oxygenated functions appended to the heterocycle system stimulate the acid catalyst, along the lone pair of the oxygen atoms of the aforementioned substituents.

These four TSAs are **TSA-1** (a pyrrolidine−nitronate), **TSA-2** (an imidazolidine−carbamate), **TSA-3** (an hexahydropyrimidine−carbamate), and **TSA-4** (an azaphosphinane−carbamate). Figure 3 shows the geometries of these TSAs while the MEPs for **TS2-A′B′** and the four proposed TSAs are depicted in Figure 4. Table 3 presents the ChelpG charges for the more relevant centers on **TS2-A′B′** and TSAs.

We have carried out a comparative geometrical analysis between the position of heavy atoms (no including hydrogen atoms) of both TSAs and **TS2-A′B′** by means of the option COMPARE of the PCMODEL program,[29] and they have been evaluated examining the root-mean-square (rms) of the atomic positions. An analysis of the results presented in Table 3 shows that the six-membered rings present a lower rms value than that of the five-membered ones, indicating that **TSA-3** and **TSA-4** are geometrically more similar to **TS2-A′B′** than the five-membered TSAs **TSA-1** and **TSA-2**. Although **TS2-A′B′** corresponds to a five-membered TS, the large C3−O6 distance in the TS increases the relative distance between the more relevant O7 and H6 centers. Moreover, a conformational analysis of **TS2-A′B′** shows that the appended group is in an axial arrangement. For the five-membered TSAs, which present a flat heterocyclic system, the appended substituents are in the same plane. However, the six-membered TSAs have the carbamate group in a pseudoaxial arrangement, due to the sp^2 hybridization of the nitrogen atom of the carbamate group. Therefore, the carbamate groups of **TSA-3** and **TSA-4** are in a similar arrangement to the carboxyl group of **TS2-A′B′**. The distance between the most negatively charged O7 oxygen atom and the most positive charged H6 hydrogen atom in each TSA provides a measure of the relative position of two of the most important recognition elements in these molecules. These distances

(29) PCMODEL V4.0, Serena Software; Bloomington, 1990.

Table 3. ChelpG Charges (au) for Selected Atoms, rms (root-mean-square) for TSAs with Respect to TS2-A′B′,[a] and H6−O7 Distances (Å)

	TS2A′B′	TSA-1	TSA-2	TSA-3	TSA-4
		ChelpG charges			
O7	−0.76	−0.60	−0.62	−0.70	−0.67
X1	1.04	0.48	0.89	1.13	1.07
X2	−0.61	0.09	−0.68	−0.82	−0.76
Y6	−0.61	−0.96	−0.65	−0.86	−0.39
H6	0.41	0.40	0.41	0.36	0.10
			rms		
		0.50	0.54	0.32	0.36
		H6−O7 distances			
	5.35	5.44	5.38	5.12	5.83

[a] X = C/N and Y = O/N/P.

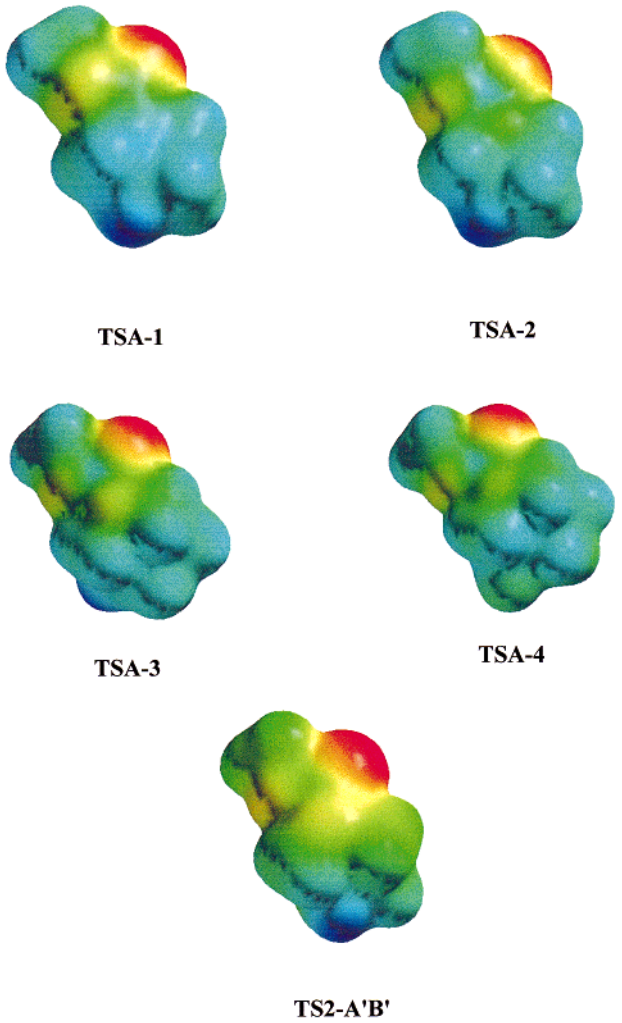

Figure 4. Electrostatic potential surface for TSAs and **TS-A′B′** (graphed over the range of −60 to +60 kcal/mol). Red area corresponds with the region where the electrostatic potential is most negative (O7), and blue is associated with the positive region (H6).

for the TSAs are in the range 5.12−5.83 Å, with that for **TSA-2** (5.38 Å) closer to that for **TS2-A′B′** (5.35 Å).

The results from the ChelpG charge calculations for **TS2-A′B′** afford high negative and positive charges at the O7 (−0.8 au) and the H6 (0.4 au) atomic centers, respectively, which correspond to the basic and acid centers that will be hydrogen-bonded to the acid and basic catalysts. The negative charge located on the O7 basic center for the four TSAs are in a narrow range,

−0.5−0.6 au, similar to that in **TS2-A′B′**. However, the positive charge located on the H6 acid hydrogen is in a wide range, 0.1−0.4 au. Other centers that can interact, X1, X2, and Y6, have been included. The small positive charge found in **TSA-4** is due to the low polarization of the P−H bond. Because of the necessity of the double catalyst to make the intramolecular Michael addition possible, the geometrically favorable **TSA-4** is defavored from the charge distribution analysis. Although the five-membered TSAs have a larger positive charge at H6, an analysis of the other selected centers points out that both **TSA-2** and **TSA-3** present similar values to those in **TS2-A′B′**. These facts, together with those obtained from the geometrical analysis, allow us to select **TSA-2** and **TSA-3** as the most favorable TSAs, since they are in line with the main factors considered above: the TSA geometry approaches the TS one and it reproduces the charge distribution on **TS2-A′B′**.

Finally, we have made a MEP analysis to compare **TS2-A′B′** and the four proposed TSAs (see Figure 4). The MEP at each point on a constant electron density surface (which approximates the van der Waals surface for each structure) is represented graphically by a range of colors: red corresponds with the regions where the electrostatic potential is most negative and blue is associated with positive regions. In the four TSAs and **TS2-A′B′**, the larger concentration of negative charge (red region) is found around the O7 oxygen atom while the larger concentration of positive charge (blue region) is found around the H6 hydrogen atom. The potential energy ranges were −64 to 81 kcal/mol for **TS2-A′B′**, −54 to 49 kcal/mol for **TSA-1**, −52 to 49 kcal/mol for **TSA-2**, −50 to 45 kcal/mol for **TSA-3**, and −49 to 25 kcal/mol for **TSA-4**.

TSA-1, **TSA-2**, and **TSA-3** present similar ranges, which are lower than that for **TS2-A′B′**, due to the charger transfer process from the O7 oxygen atom to the carboxyl group in the latter. As can be observed, the electrostatic potentials of these three TSAs closely resemble that of **TS2-A′B′**. Therefore, they should be able to duplicate the electrostatic interactions of the **TS2-A′B′**. **TSA-4** can be discarded as a possible TSA due to the low acid nature of the P−H bond responsible for the low value of the positive MEP.

Interestingly, to test the results obtained in this theoretical study, developing the experimental synthesis of the proposed TSA will be the next step in this research line.

Conclusions

In the present paper, we have carried out a theoretical study to design appropiate transition state analogues for the intramolecular Michael addition of methyl 2-(2-hydroxyethyl)acrylate to give the unexpected tetrahydrofuran derivative. First, we have studied the two reactive channels in basic medium to give the direct (1,2 addition) and the Michael (1,4 addition) adducts. This study allows us to assert that the strains that appears along the intramolecular 1,4 attack are responsible for the large energy relative to the 1,2 one, in agreement with Baldwin's rules. Second, the inclusion of acid/base residues acting as catalysts are analyzed and the different shape of the corresponding TSs open the possibility of discrimating the disfavored 1,4 addition reaction, instead of the favored 1,2 one, by the design of an appropriate TSA. A comparison of the geometrical parameters, charge distribution, and molecular electrostatic potential among the TS for the intramolecular 1,4 addition and the four proposed TSA candidates allows us to select an imidazolidine−carbamate and a hexahydropyrimidine−carbamate as the more appropriate ones.

Acknowledgment. This work was supported by research funds provided by the Conselleria de Cultura Educació i Ciéncia, Generalitat Valenciana (Project GV97-CB-11-96). All calculations were performed on a Cray-Silicon Graphics Origin 2000 with 64 processors of the Servicio de Informática de la Universidad de Valencia. We are most indebted to this center for providing us with computer capabilities.

JO991117C